Computers in Railways V
Volume 2: Railway Technology and Environment

Editors: J. Allan, C.A. Brebbia, R.J. Hill,
G. Sciutto, S. Sone

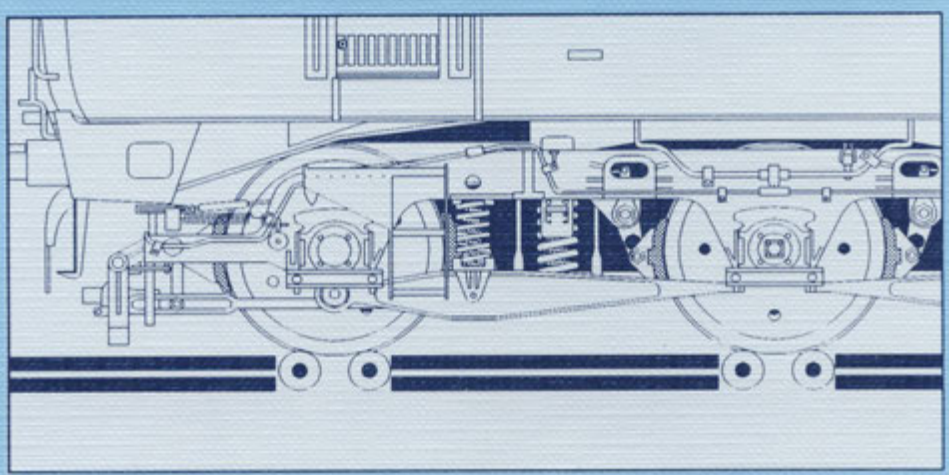

Computational Mechanics Publications

Computers in Railways V - Volume 2

Railway Technology and Environment

EDITORS:

J. Allan
The University of Birmingham
& London Underground Ltd, UK

C.A. Brebbia
Wessex Institute of Technology, UK

R.J. Hill
University of Bath, UK

G. Sciutto
Università Degli Studi di Genova, Italy

S. Sone
The University of Tokyo, Japan

Computational Mechanics Publications
Southampton Boston

CONTENTS

Design of wagon wheels using the Finite Element Method

V. Yessaulov, Y. Taran, A. Sladkozsky, A. Kozlovzsky, N. Shmurygin
State Metallurgical Academy of Ukraine, Dnepropetrovsk, Ukraine

Abstract

The finite element method was employed for developing new designs of railroad car wheels. The problem was formulated in general terms, the region at hand discretized, and the contact problem and the heat conduction problem were solved for which the boundary conditions were assigned. The numerical solution error was determined. Mathematical modeling of various wheel designs was carried out, and CAD-enhanced wheels were rolled. The effectiveness of the new wheel designs was validated in service tests.

1 Introduction

The railroads are responsible for the major part of loads carried in the Newly Independent States. No high-speed transportation exists in the region, and the majority of merchandise is transported by heavy-load railroad stock (up to 25 t per axle). Hence, the use of appropriate locomotive and car wheels. The local service conditions have to be taken into account in designing the wheels. For various reasons, side wear of wheel tread, particularly in the flange area, increased greatly during the past decade. The designers' efforts therefore were aimed at extending the durability of the wheels and of the permanent way alike.

For mathematical modeling of wheel-rail interactions and analysis of state of strain and stress in the wheel, an initial graphical representation of wheel was needed. AutoCAD version 13.0 was used for this purpose. Wheel radial section contour was set as a starting polyline. A special LISP program converted this image to a numerical form usable in the rest of the software.

2 Finite element problem statement

Semi-analytical FEM was used to study the state of stress in the wheel. As is well-known, this approach permits reducing a three-dimensional problem of the theory of elasticity to a set of two-dimensional problems for an arbitrary nth harmonic. For instance, the nodal displacement vector in the ith node may be written in cylindrical coordinates r, z, θ, where z axis corresponds to the wheel axis, as

$$\{\Delta_i\} = \sum_{n=0}^{N} [\Omega^n] \{\Delta_i^n\} \tag{1}$$

N being the number of the Fourier series terms. The $[\Omega^n]$ matrix and the $\{\Delta_i^n\}$ vector are defined as

$$[\Omega^n] = \begin{bmatrix} \cos n\theta & 0 & 0 \\ 0 & \cos n\theta & 0 \\ 0 & 0 & \sin n\theta \end{bmatrix} \tag{2}$$

$$\{\Delta_i^n\} = \begin{Bmatrix} \Delta_{ir}^n \\ \Delta_{iz}^n \\ \Delta_{i\theta}^n \end{Bmatrix} \tag{3}$$

Neglecting the damping and the gravitational force, one can write a resolvent matrix differential equation for the nth harmonic in the form

$$[K^{nn}]\{\Delta^n\} + [M^{nn}]\frac{\partial^2}{\partial t^2}\{\Delta^n\} = \{F^n\} \quad , \qquad n = 0,1,\ldots,N \tag{4}$$

The following expressions hold that use Zenkevich's results [1]:

$$[K^{nn}] = \iiint_V [B^n]^T [D][B^n] dV \tag{5}$$

$$[M^{nn}] = \rho \iiint_V [A^n]^T [A^n] dV \tag{6}$$

Here, $[A^n]$ is the form function matrix for the nth harmonic, $[D]$ the elastic property matrix for the wheel steel, $[B^n]$ the matrix accounting for the wheel geometry, ρ the steel density. The vector $\{F^n\}$ takes into account the surface loads and the effects of temperature fields developing in the wheel during braking.

The discretization of the region at hand is performed using axisymmetric simplex elements with triangular cross sections. The resultant division is displayed on the computer monitor and can be changed at will. Slender extended elements are thereby eliminated which is important for an accurate solution, especially in the wheel plate area. The matrices of rigidity, of elastic properties etc. are generated via a standard assembling procedure, and

boundary conditions are assigned. Among other things, the wheel temperature profiles are to be determined.

3 Solution of the heat conduction problem

The dynamics of wheel temperature change and that of contact interactions are incommensurable, so a distinct problem of heat conduction was solved to determine the temperature fields. A matrix differential equation of heat conduction was given e.g. by Zarubin [2]:

$$[C]\left\{\dot{T}\right\}+[\Lambda]\{T\}=\{Q\} \tag{7}$$

where $\{T\}$ is the k-dimensional vector of nodal temperatures, k the number of grid nodes, $\left\{\dot{T}\right\}$ the corresponding vector of derivatives of the temperatures with respect to time, $\{Q\}$ the vector of heat fluxes directed to the boundary nodes. $[C],[\Lambda]$ are the $k\times k$ matrices of heat capacity and thermal conductivity respectively. The two matrices are time-dependent, for there is a temporal change in the temperature field changes for a nonstationary problem. Hence, the heat capacity and thermal conductivity of the wheel steel are variable quantities.

To generate the matrices, empirical equations relating the heat capacity and the thermal conductivity of the wheel steel to local temperature were developed. The heat transfer from the wheel sides was neglected for the time interval at hand. The thermal flux due to contact of brake shoes with the wheel was assumed to be constant. This approach allowed to solve eqn (7) by use of a three-layer difference technique in which the coefficients in $[C],[\Lambda]$ are determined from the nodal temperatures at the instant $t_{\omega-1}$ corresponding to the middle of a doubled time interval $2\Delta t=t_{\omega}-t_{\omega-2}$. The two matrices then are assigned a time index of $\omega-1$, that is $[C]_{\omega-1},[\Lambda]_{\omega-1}$. Therefore, eqn (7) may be rewritten in a finite difference form as

$$\left(1{,}5\frac{[C]_{\omega-1}}{\Delta t}+[\Lambda]_{\omega-1}\right)\{T\}_{\omega}=1{,}5\frac{[C]_{\omega-1}\{T\}_{\omega-2}}{\Delta t}-$$

$$-[\Lambda]_{\omega-1}\left(\{T\}_{\omega-1}+\{T\}_{\omega-2}\right)+3\{Q\} \tag{8}$$

Assuming that the temperature fields at the instants $\omega-2$, $\omega-1$ are determined and, consequently, so are $[C]_{\omega-1},[\Lambda]_{\omega-1}$ and the vector $\{Q\}$, eqn (8) can be regarded as a typical matrix equation for $\{T\}_{\omega}$ and reduced to a set of k linear algebraic equations. The initial conditions of Cauchy problem are apparent, i.e. $\{T\}_{-1}$, $\{T\}_{0}$ are null vectors.

k linear algebraic equations. The initial conditions of Cauchy problem are apparent, i.e. $\{T\}_{-1}$, $\{T\}_0$ are null vectors.

To solve the heat conduction problem, a distinct program module was written which calculated the wheel temperature fields at any instant of braking. The time quantum was taken to be 1 s.

4 Wheel-rail interactions

Both dynamic and quasistatic formulation of the problem was considered. To do this, analysis of a simplified model of interactions was performed. The track-wheel-vehicle system was assumed to be a three-mass dynamic system, and temporal relationships for the dynamic forces acting on the wheel in various rough sections of track or arising due to the wheel's tread defects were determined.

Suppose that both vertical P and horizontal Q force exerted on the wheel are known from the solution of the above problem. The task is to determine the state of stress in the near-contact zone of the wheel. With this in mind, interactions in the wheel-rail system were considered. The wheel-rail contact was simulated by FEM using simplified models of two-dimensional interaction. For purposes of design, however, quasi-Hertzian approach to simulation was preferred.

Let the profiles of the interacting wheel and rail be assigned in some way. (One of the ways to assign wheel tread profile $f(x)$ in service was by scanning its contour which next was interpolated by computer.) First, conditions of negotiation of track are examined for the wheelsets and the entire truck, and current relative position of the wheel and rail is determined. In doing so, tilt of the rail, dynamic detilting of the rail, and deformations of other elements are taken into account. To determine contact stresses after Hertz, one should find the initial contact point. For this, a three-dimensional problem of minimization of a functional, namely of the vertical distance between the wheel surface and the rail surface, is considered. Numerical treatment of this problem includes contemplation of vertical distances h_i over the array of FEM grid nodes of the wheel and rail lying in the contact region. When the point is found, the principal curvatures of the contacting surfaces are determined from the solution of characteristic equation. Next, the semiaxes of the contact ellipse can be found. Clearly, Hertz distribution of stresses takes place within the contact zone.

This approach is justified under conventional assumptions of contact problems only when a single-zone contact occurs in the wheel/rail pair. Yet wheelset hunting may lead to two-zone contact. Suppose that analysis of the h_i distances may yield two local minima h_{m1}, h_{m2} corresponding to a possibility of two-zone contact. It is clear that for any actual wheel and rail profiles two

wheel points will correspond to two minima, one in the flange region and one on the tread. If a vertical force $P_1 < P$ is assumed to act in the first zone, then a vertical force $P_2 = P - P_1$ is exerted in the second zone. It should be noted that a total force normal to the contacting body surface is used in Hertzian theory equations. Under the assumption of smooth surfaces, this force for the *i*th zone

$$N_i = P_i \sqrt{1 + \left(\frac{\partial f}{\partial x}\right)_i^2} \tag{9}$$

where the derivative $\frac{\partial f}{\partial x}$ is defined in the corresponding *i*th point of contact.

Following Ponomarev et al. [3], one can find the normal convergence of the wheel and rail surfaces in the *i*th contact zone

$$\delta_i = \frac{1}{2} n_\delta \sqrt[3]{9 \left[\frac{(1-\nu^2)N_i}{E}\right]^2 \Sigma k} \tag{10}$$

where it is assumed that the moduli of elasticity E and the Poisson's ratios ν are equal for the wheel and the rail, Σk is the total of principal curvatures of the surfaces of wheel and rail determined in the *i*th contact point, and n_δ is a tabulated coefficient dependent on the principal curvatures. It is essential that the vertical convergencies of the surfaces in the contact zones have the same value considering the distances between the surfaces prior to interaction, that is

$$\frac{\delta_1}{\sqrt{1 + \left(\frac{\partial f}{\partial x}\right)_1^2}} + h_{m1} = \frac{\delta_2}{\sqrt{1 + \left(\frac{\partial f}{\partial x}\right)_2^2}} + h_{m2} \tag{11}$$

Equation (11) is the governing relationship for iterative search of forces P_i and consequently all other parameters enabling evaluation of the existence, location and dimensions of each contact zone and calculation of contact stresses. Figure 1 depicts a graphic output of computer simulation of contact interaction between a wear-free wheel having a standard GOST 9036-88 profile, and an R65 rail.

It is seen from fig. 1 that two contact zones exist. The central zone has a nearly circular shape while the flange one is shaped as an elongated ellipse and leads the central zone at a nonzero angle of attack. The side captions refer to calculation conditions where "sm" denotes the wheelset displacement relative to the track, "alpha" the angle of attack of the wheelset, "S" the total area of the contact zones, "s1, s2" the contact stresses in the 1st and the 2nd contact zone respectively. Clearly, the contact stress values in the flange zone are such that plastic deformations can and do set on, leading to rapid thinning of flange and eventually to sharp flange.

To prevent such defects which cause massive economic losses associated with wheelset reconditioning, assessment of performance of a variety of wheel

designs, including those with the AAR and the UIC treads was undertaken. Based on these studies, alternative tread profiles for car and locomotive wheels and asymmetric head profiles for rails were developed. A 1.3 to 2-fold reduction in wheel flange wear rate was achieved due to their introduction at line and in-plant railroads.

5 Boundary conditions

Boundary conditions have to be formulated and vector $\{F^n\}$ assigned to solve eqn (4). Let following distributed loads act on the wheel surface: normal one, $p(s,\theta)$; tangential one directed along the generating line, $q(s,\theta)$; and tangential one perpendicular to the generating line, $t(s,\theta)$. The coordinate s is the arc distance measured along the tread generating line. Let us divide the contact region to bands $s_i \le s \le s_{i+1}$ by use of circumferences $s = s_0, s = s_1, \ldots, s = s_j$ whose subscripts correspond to their respective contact node numbers i. Integrating the surface loads p, q, t within each band, one can approximate each of the loads with a unique singulary function $p_i(\theta), q_i(\theta), t_i(\theta)$. The components of vector $\{F^n\}$ in the ith node can be written as

$$\{F_i^n\} = \pi r_i l_i \begin{Bmatrix} p_i^n \cos\alpha_i - q_i^n \sin\alpha_i \\ p_i^n \sin\alpha_i + q_i^n \cos\alpha_i \\ t_i^n \end{Bmatrix} , \qquad n = 1,2,\ldots,N \tag{12}$$

$$\{F_i^0\} = 2\pi r_i l_i \begin{Bmatrix} p_i^0 \cos\alpha_i - q_i^0 \sin\alpha_i \\ p_i^0 \sin\alpha_i + q_i^0 \cos\alpha_i \\ 0 \end{Bmatrix} , \qquad n = 0 \tag{13}$$

Here, l_i is the length of arc $s_i \le s \le s_{i+1}$, α_i the angle between the radius r_i and the normal to the contact surface at the ith node, p_i^n, q_i^n, t_i^n the coefficients of the Fourier series for the loads, e.g.

$$p_i^n = \frac{1}{\pi} \int_{-\pi}^{\pi} p_i(\theta) \cos n\theta \, d\theta , \qquad n = 1,2,\ldots,N \tag{14}$$

$$p_i^0 = \frac{1}{2\pi} \int_{-\pi}^{\pi} p_i(\theta) \, d\theta \tag{15}$$

Turning back to the contact stresses obtained by the algorithm described in the previous section, one can write the stresses $p_i(\theta)$ in the band $s_i \le s \le s_{i+1}$ as

$$p_i(\theta) = \sigma_i \sqrt{1 - \left(\frac{\theta}{\theta_i}\right)^2} \tag{16}$$

where θ_i is the angular boundary of the ith band, σ_i the maximum contact stresses in the band allowing for interpolation. It follows from eqns (14) and (15) that

$$p_i^0 = \frac{1}{2\pi}\int_{-\theta_i}^{\theta_i} \sigma_i \sqrt{1-\left(\frac{\theta}{\theta_i}\right)^2}\, d\theta = \frac{\sigma_i \theta_i}{4} \tag{17}$$

$$p_i^n = \frac{1}{\pi}\int_{-\theta_i}^{\theta_i} \sigma_i \sqrt{1-\left(\frac{\theta}{\theta_i}\right)^2} \cos n\theta\, d\theta = \frac{\sigma_i}{n} J_1(n\theta_i), \quad n = 1,2,\ldots,N \tag{18}$$

J_1 in eqn (18) is Bessel's function of the first kind. To eliminate shift of the region at hand as a rigid whole, some boundary conditions were assigned in displacement form. For example, radial displacement u was assumed at the inner hub surface,

$$u = \frac{pd}{2E}\left(\frac{1+k^2}{1-k^2} + \nu\right) \tag{19}$$

k being the ratio of the inner hub diameter d to the outer one. Following formula was used to obtain the average fit pressure:

$$p = \frac{E\delta}{d\left[\lambda(1-\nu) + \left(\frac{1+k^2}{1-k^2} + \nu\right)\right]} \tag{20}$$

where δ is the processing interference during pressing of wheel into axle, λ the coefficient dependent on the ratio of the loaded section length to the axle diameter and equal to the ratio between the actual average displacement and the displacement determined after Lamé.

Thus the problem of the state of stress and strain in a railroad wheel was stated in a finite element form. Furthermore, the accuracy of finite element solution was assessed. For this purpose, analytical solutions were obtained by function theory techniques for a flat-plate wheel. Finite element discretization was performed and a numerical solution found for a similar wheel. Comparison of the results yielded finite element grid parameters and the number of terms in the Fourier series needed to maintain the solution accuracy within 5%.

6 Development of new wheel designs, and service tests

Various wheel designs were simulated, and stress fields in diverse radial sections of the wheels obtained. For example, fig. 2 depicts stress field in the lower radial section of standard wheel now in use at railroads of Ukraine, Russia and some other countries. Consideration is being given to the wheel's position on the rail when only one contact zone exists which is located in the middle of the thread. The lateral force exerted on the wheel is negligible. No braking action is taken. The stress level in any area of wheel section is represented by the density of gray. The maximum and the minimum stress are

both located in the region of transition from the hub to the plate. The distortion of the section also is shown (in exaggerated form).

The work has resulted in development of several new wheel designs featuring stresses 10-20 % below those of any counterparts now in service. The wheels were rolled at the Nizhnedneprovsk Tube and Pipe Plant (Dnepropetrovsk, Ukraine). They demonstrated improved reliability in tests conducted at line and in-plant railroads in Ukraine and Russia. Nev'yansk Mechanical Works (Russia) makes tools for reprofiling the wheel threads to the alternative contours. Less severe wear was observed on the new design wheels in heavy-load service. This trend was particularly striking in transportation of rock in the mining industry where loads on axle may reach 30 t and above. A more than 2-fold extension of wheel service life was reportedly achieved e.g. at Mikhailovo Mining and Beneficiation Plant (Russia). Metallographic characterization of steel in as-delivered and test-run wheels alike validated the estimated stress lowering due to the new designs.

The methodology developed in the study is applicable for simulation of wheel-rail interactions in rapid transit systems. Improved tread profiles and wheel designs are to be devised in the course of further R&D aimed to meet the requirements of high-speed trunk lines currently developed in Ukraine and Russia.

References

1. Zienkiewicz, O.C. *The Finite Element Method in Engineering Science*, McGraw-Hill, London, 1971. (Russian translation, 1975).
2. Zarubin, V.S. *Applied Problems of Structural Element Thermal Strength*, Mashinostroenie, Moscow, 1985. (In Russian).
3. Ponomarev, S.D., Biderman, V.L. & Likharev, K.K. *Strength Analysis in Engineering, Vol. 2*, Mashgiz, Moscow, 1958. (In Russian).

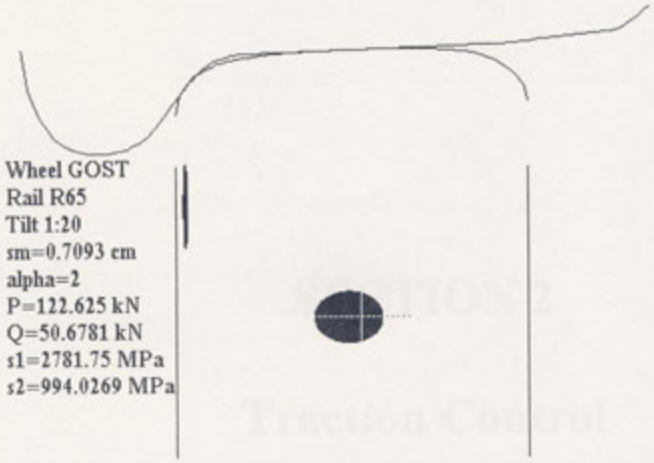

Figure 1: Results of computer simulation of wheel/rail contact interaction. Wheel to GOST 9036-88, rail R65, tilt of the rail = 1:20, sm = 0.7093 cm, alpha = 2 degrees, P = 122.625 kN, Q = 50.6781 kN, s1 = 2781.75 MPa, s2 = 994.0269 Mpa.

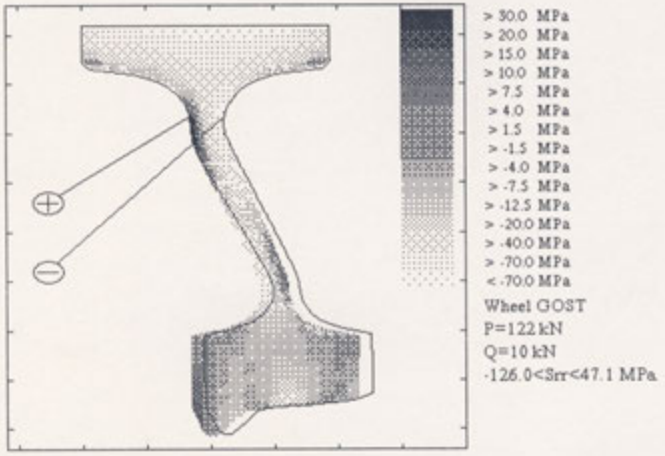

Figure 2: Stress field σ_{rr} in a lower radial section of a GOST 9036-88 wheel. P = 122 kN, Q = 10 kN, -126.0<Srr<47.1 MPa.